

don, 1900; reprinted by Dover Publications, Inc., New York, 1961), Part II, p. 27.

<sup>39</sup>M. Hamermesh, *Group Theory* (Addison-Wesley Publishing Co., Inc., Reading, Mass., 1962), Chap. 1.

<sup>40</sup>L. Mandel, *J. Opt. Soc. Am.* **51**, 1342 (1961); Ref. 20, Sec. 5.5.

<sup>41</sup>Reference 20, Eq. (6.23).

<sup>42</sup>F. Davidson and L. Mandel, *Phys. Letters* **27A**, 579 (1968).

<sup>43</sup>D. Slepian, *Bell System Tech. J.* **37**, 163 (1958).

<sup>44</sup>I. S. Gradshteyn and I. M. Ryzhik, *Table of Integrals, Series, and Products* (Academic Press Inc., New York, 1965), p. 19.

## Hyperfine Structure of Bi<sup>209</sup>

Robert J. Hull\* and Gilbert O. Brink

*Department of Physics and Astronomy, State University of New York, Buffalo, New York 14214*

(Received 8 July 1969)

We have used the atomic-beam magnetic-resonance technique to improve and extend the measurements of Title and Smith on the hyperfine structure of the  $(6p^3)^4S_{3/2}$  ground state of Bi<sup>209</sup> ( $I = \frac{9}{2}$ ). We measured the three zero-field hyperfine intervals and computed the octupole interaction constant. Our experimental results are  $\nu_1(F=5 \rightarrow F=6) = 2884.666(2)$ ,  $\nu_2(F=4 \rightarrow F=5) = 2171.419(2)$ , and  $\nu_3(F=3 \rightarrow F=4) = 1584.502(2)$  MHz. From these values, we obtain for the hyperfine-interaction constants, corrected for the pseudo-octupole interactions due to perturbation by neighboring fine-structure levels  $A = -446.937(1)$ ,  $B = -305.067(2)$ , and  $C = 0.0183(1)$  MHz. The assigned errors include only the experimental errors in the measurement of the three hyperfine intervals, and no estimate of the errors in the theoretical corrections has been made. We have also corrected the data of Lurio and Landman for the  $(6p^3)^2P_{3/2}$  metastable state of bismuth for these octupolelike interactions and have deduced a fairly consistent value for the one-electron octupole-interaction constant. From the average value of the octupole-interaction constant  $c_{3/2} = 0.0206$  MHz we find that the nuclear magnetic octupole moment is  $0.0086\mu_N$ . This value is compared with the prediction of the shell model.

### I. INTRODUCTION

In the course of a series of experiments designed to observe the hyperfine structure of the metastable electronic states of the  $(6p^3)$  configuration of bismuth we found that, due to the focusing properties of our atomic-beam apparatus, we could observe directly at least one transition in each of the  $\Delta F = 1$  hfs intervals of the  $^4S_{3/2}$  ground state. We measured the frequencies as accurately as possible in order to observe the octupole interaction in this state of bismuth. The results of these measurements are presented in this paper.

The hyperfine structure in the ground state of Bi<sup>209</sup> was studied by Title and Smith,<sup>1</sup> who were able to observe two of the direct transitions and were able to assign values to the hyperfine-interaction constants  $A$  and  $B$ . We have decreased the uncertainty in their values and have been able to obtain a value for  $C$ . This has been possible primarily because of our signal averaging system which allows the resonances to be observed with a good signal-to-noise ratio and, thus, allows the determination of the transition frequencies with small uncertainties.

Lurio and Landman<sup>2</sup> have made precise measurements of the hfs and  $g$  factors of metastable states in the ground electronic configuration of bismuth. We have freely used the results of their analysis of this configuration in our own work.

In this paper, we give a brief introduction to the theory of hfs, a description of our apparatus, and our results and interpretation. In the Appendix we present the matrix elements required to remove the octupolelike contributions of the dipole and quadrupole interactions to the hyperfine structure.

### II. THEORY

In order to fix our notation, we summarize the main formulas used in the theory of hyperfine structure. The relevant Hamiltonian, valid for matrix elements diagonal in  $J$ ,  $L$ , and  $S$ , is

$$\begin{aligned} \mathcal{H}_{\text{hfs}} = & A \vec{I} \cdot \vec{J} + B Q_{\text{op}} + C \Omega_{\text{op}} \\ & - g_J \mu_B H_J^z - g_I \mu_N H_I^z, \end{aligned} \quad (1)$$

where  $\vec{I}$  and  $\vec{J}$  are the nuclear spin and total electronic angular momentum operators, respectively;

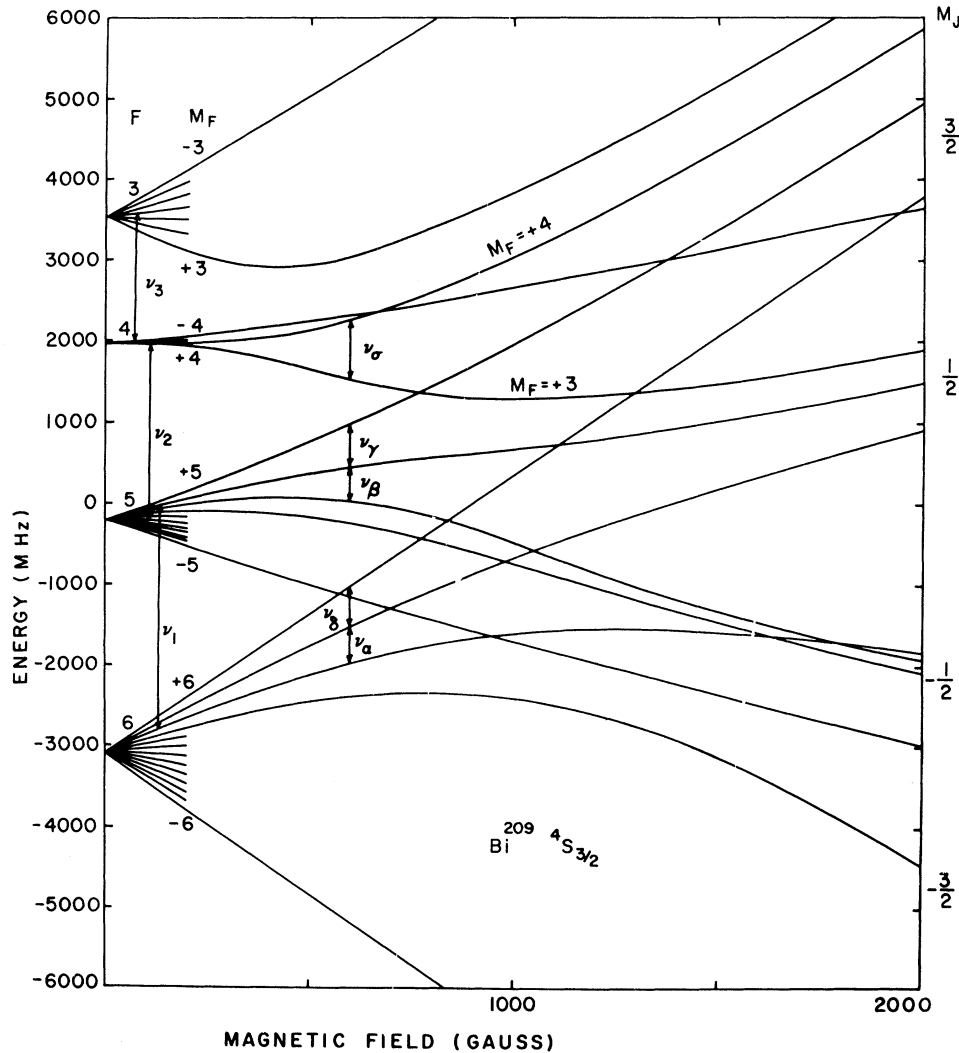


FIG. 1. Zeeman effect of the ground state of  $\text{Bi}^{209}$  ( $I = \frac{9}{2}$ ). The hfs is inverted in this state. The low-frequency transitions focusable in our apparatus are indicated by arrows and Greek subscripts.

$A$ ,  $B$ , and  $C$  are, respectively, the magnetic-dipole, electric-quadrupole, and magnetic-octupole hyperfine-interaction constants;  $g_J$  is the electronic  $g$  factor, which in our convention is a negative quantity for the ground state of bismuth;  $\mu_B$  and  $H$  are the Bohr magneton and the external magnetic-field strength; and  $g_I = \mu_I/(\mu_B I)$  is the nuclear  $g$  factor.

In the absence of an externally applied magnetic field, an atomic state with a particular value of  $J$  splits into either  $(2I+1)$  or  $(2J+1)$  levels, whose energies depend on the values of the hyperfine-interaction constants and the quantum numbers  $I$ ,  $J$ , and  $F$ , where  $F$  is the total angular momentum of the level. To first order in perturbation theory the magnetic-dipole hyperfine energy is

$$W_F^{(1)} = \frac{1}{2} A [F(F+I) - I(I+1) - J(J+1)]. \quad (2)$$

Similar expressions<sup>3</sup> can be found for the quadrupole and octupole terms. Figure 1 is a plot of these energy separations as a function of magnetic field for the ground state of  $\text{Bi}^{209}$  ( $I = \frac{9}{2}$ ), the pattern being inverted for this state.

The atomic-beam apparatus is used to measure transition frequencies between energy levels characterized by the quantum numbers  $F$  and  $M_F$ . The hyperfine-interaction constants can be obtained most accurately when the direct transitions, that is, transitions between states of different  $F$ , are measured. At zero external magnetic field, these energy differences are given to first order in perturbation theory by:

$$\begin{aligned} \nu_1 &= (W_6 - W_5)/h = 6A + \frac{2}{3}B + \frac{16}{9}C, \\ \nu_2 &= (W_5 - W_4)/h = 5A - \frac{5}{24}B - \frac{65}{6}C, \\ \nu_3 &= (W_4 - W_3)/h = 4A - \frac{2}{3}B + \frac{208}{27}C. \end{aligned} \quad (3)$$

Since the dipole- and quadrupole-interaction energies in second-order perturbation theory are comparable in magnitude to the first-order octupole energy, the off-diagonal matrix elements of these operators must be calculated in order to obtain the true octupole-interaction constant. This is done best by expressing the hyperfine-structure Hamiltonian (without an external magnetic field) in terms of tensor operators of rank  $k$ :

$$\mathcal{H}_{\text{hfs}} = \sum_k [\sum_i T_e^{(k)}(i)] \cdot T_n^{(k)} \quad (4)$$

$$\begin{aligned} W_F^{(2)} &= \sum_{(\alpha'J')} \langle \beta I \alpha J F M | \mathcal{H}_{\text{hfs}} | \beta I \alpha' J' F M \rangle^2 [W(\alpha J) - W(\alpha' J')]^{-1} \\ &= \sum_{(\alpha'J')} \left[ \sum_{k=1}^2 \left\{ \begin{matrix} F & I & J' \\ k & J & I \end{matrix} \right\} \langle \beta I | T_n^{(k)} | | \beta I \rangle \langle \alpha J | \sum_i T_e^{(k)}(i) | | \alpha' J' \rangle \right]^2 \\ &\quad \times [W(\alpha J) - W(\alpha' J')]^{-1} \quad , \end{aligned} \quad (5)$$

where  $[W(\alpha J) - W(\alpha' J')]$  is the energy difference of the fine-structure states  $\alpha J$  and  $\alpha' J'$ . The zero-order wave function  $|\beta I \alpha J F M\rangle$  is characterized by the quantum numbers  $I, J, F$ , and  $M$ , and by any other nuclear ( $\beta$ ) or electronic ( $\alpha$ ) quantum numbers needed to specify the state completely. The prime on the summation means that  $\alpha' J' \neq \alpha J$ . The reduced matrix elements of the operator  $T_n^{(k)}$  are proportional to the nuclear moments, while the reduced matrix elements of  $T_e^{(k)}(i)$  are proportional to one-electron hyperfine-interaction constants which are identified by lower-case letters:  $a$  for the dipole constant,  $b$  for the quadrupole, and  $c$  for the octupole. The definitions of the single-electron reduced matrix elements are given by Lurio, Mandel, and Novick.<sup>4</sup>

In bismuth, the coupling of the  $p$  electrons is intermediate between  $LS$  and  $jj$ , and the three states with  $J = \frac{3}{2}$  are expressed as linear combinations of the  $LS$ -coupled states. The  $LS$ -coupling coefficients,  $a_s, a_p$ , and  $a_d$ , are obtained by fitting the experimental fine-structure energy separations to theory, as explained in the Appendix. The  $a$ 's are transformed then to the  $jj$ -coupling set of coefficients  $c_{ij}$  for use in evaluating the single-electron matrix elements. Both sets of coefficients are included in Table I and are the ones given by Lurio and Landman.<sup>2</sup>

Finally, we list for completeness the diagonal elements of the hyperfine-structure interactions in terms of the one-electron constants. These expressions appear in Lurio and Landman,<sup>2</sup> and we have verified their correctness:

$$A(^2D_{5/2}) = \frac{4}{5}a' + \frac{1}{5}a'' \quad , \quad A(^2P_{1/2}) = a'' \quad ,$$

$T_e^{(k)}(i)$  and  $T_n^{(k)}$  operate on the spaces of electron and nuclear coordinates, respectively. The summation on  $i$  is over all the electrons. The index  $k$  takes on values 1, 2, and 3 for the dipole, quadrupole, and octupole interactions, respectively. The identification of the tensor operators with the conventional interaction constants  $A, B$ , and  $C$  is made explicitly by Schwartz.<sup>3</sup> If we write the energy of a state  $F$  to second order as  $W_F = W_F^{(1)} + W_F^{(2)}$ , then the second-order term becomes

$$\begin{aligned} A(J = \frac{3}{2}) &= a'(1 + \frac{1}{5}c_{2i}^2) - \frac{1}{5}a''c_{2i}^2 \\ &\quad - 4(\frac{2}{5})^{1/2}c_{2i}(c_{1i} - c_{3i})a''' \quad , \end{aligned} \quad (6)$$

$$B(^2D_{5/2}) = B(^2P_{1/2}) = 0 \quad ,$$

$$B(J = \frac{3}{2}) = b_{3/2} [c_{3i}^2 - c_{1i}^2 - 2c_{2i}(c_{1i} + c_{3i})(\frac{2}{5})^{1/2}\eta] \quad ,$$

$$C(^2D_{5/2}) = 2c_{3/2} \quad ,$$

$$C(J = \frac{3}{2}) = c_{3/2}(c_{1i}^2 - 4c_{2i}^2/5 + c_{3i}^2) \quad .$$

The contribution of the dipole and quadrupole terms in second order can be obtained from the matrix

TABLE I. Intermediate coupling coefficients.<sup>a</sup> The  $c$ 's are the coefficients in  $jj$  coupling, while the  $a$ 's are the  $LS$ -coupling coefficients.

	<sup>4</sup> S <sub>3/2</sub>	<sup>2</sup> D <sub>3/2</sub>	<sup>2</sup> P <sub>3/2</sub>
$c_{1i}$	0.1733	-0.0655	0.9826
$c_{2i}$	-0.3104	0.9430	0.1184
$c_{3i}$	-0.9345	-0.3264	0.1433
$a_{si}$	0.7536	-0.5799	0.3074
$a_{di}$	0.3769	0.7662	0.5213
$a_{pi}$	-0.5382	-0.2772	0.7961

<sup>a</sup>Values shown are taken from Ref. 2.

elements given in the Appendix. Second-order effects of the octupole operator are assumed to be negligible.

### III. APPARATUS

The atomic-beam magnetic-resonance apparatus employed for this research uses a six-pole *A* magnet and a two-pole *B* magnet, which are similar in design to the magnets used by the atomic-beam group at Princeton University.<sup>5</sup> The *A* magnet produces a magnetic field that has radial symmetry and a large gradient which increases outwards from the axis of the apparatus. Atoms with an effective magnetic moment  $\mu_{\text{eff}} < 0$  are deflected toward the axis, while atoms with a positive effective moment are deflected outward. This magnet is adjusted so that most of the atoms that pass through it and can enter the entrance slit of the *B* magnet must have  $\mu_{\text{eff}} < 0$ .

The *B* magnet has the property of deflecting atoms with  $\mu_{\text{eff}} < 0$  downward in Fig. 2 and atoms with  $\mu_{\text{eff}} > 0$  upward. Thus, most atoms entering the *B* magnet, which have not been disturbed in the *C*-magnet region, are deflected into the pole tips and cannot pass through the *B*-magnet exit slit. The exit slit forms the only stop that lies on the axis of

the apparatus. Both the *A* and *B* magnets are permanent magnets and are located within the vacuum envelope of the machine. This procedure results in a less complex, as well as a more stable, system than one using electromagnets. The magnetic field has a maximum value of about 8 kG in each magnet. The *C* magnet is a 4-in. electromagnet and is located outside the vacuum envelope.

A typical trajectory through the apparatus is shown in Fig. 2. Here the solid lines represent atoms that have undergone a "flop-in" transition. For most atomic-beam machines, the focusing condition for a flop-in transition requires that, for an odd *Z* atom, the high magnetic-field quantum number  $M_J$  change between the states  $M_J = \frac{1}{2}$  and  $M_J = -\frac{1}{2}$  in the *C*-magnet region. In our apparatus, atoms which enter the *A* magnet with  $M_J = +\frac{3}{2}$  can be over-focused toward the axis of the apparatus. In such a case a transition to  $M_J = +\frac{1}{2}$  induced in the *C*-magnet region will force atoms to be driven away from the poles of the *B* magnet and through the exit slit into the detector. This behavior has been verified both experimentally and through detailed numerical calculations which show an appreciable effective solid angle for transitions of the type  $M_J = \frac{3}{2} \rightarrow M_J = \frac{1}{2}$ . This behavior is illustrated by the dashed trajectory in Fig. 2. Hence, we have been

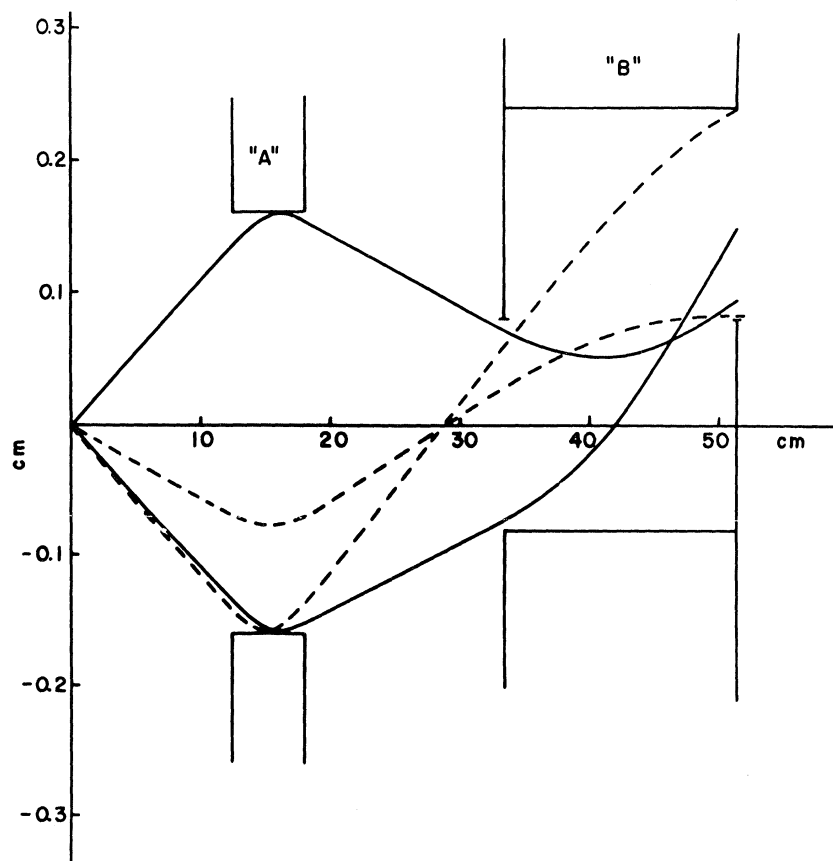


FIG. 2. Typical flop-in trajectories through our apparatus. The solid lines indicate the paths of atoms which undergo the conventional  $M_J = +\frac{1}{2} \rightarrow M_J = -\frac{1}{2}$  transition. The paths of atoms which undergo the  $M_J = +\frac{3}{2} \rightarrow M_J = +\frac{1}{2}$  transition are shown by the dashed lines.

able to detect the additional transition ( $\nu_3$  in Fig. 1) required to measure all three  $|\Delta F|=1$  hyperfine intervals in bismuth. Incidentally, our experimental observation of this transition ( $\nu_3$ ) is further verification that the hyperfine structure in the ground state is inverted.<sup>6</sup>

The beam of atomic bismuth was produced in a snouted tantalum oven similar in design and dimensions to that used by Title and Smith. The electron-bombardment current used to heat the snout was electronically regulated in both voltage and current to stabilize the bismuth beam. A satisfactory beam was produced with an input power to the oven of about 65 W. At this power, the snout temperature was approximately 1500 °C.

The bismuth beam is detected by means of electron-bombardment ionization followed by mass analysis with a Paul mass filter and an electron multiplier. Details of the ionizer and mass filter have been described by Brink.<sup>7</sup> The output of the electron multiplier is amplified by means of a Keithley Model 417 picoammeter. The signals are enhanced by repeatedly scanning through the resonance condition and accumulating the data in a Nuclear Data 1024-channel pulse-height analyzer used in the time-sequence scaling mode. The mode of operation and expected signal enhancement are similar to those described by Klein and Barton.<sup>8</sup> Either magnetic field or frequency can be swept in our system.

The radio frequency equipment consists of a Frequency Electronics, Inc., Model FE101A, frequency standard driving a General Radio Model 1164-A frequency synthesizer capable of a maximum frequency of 69.9 MHz. This frequency is then multiplied up to a factor of 8 by appropriate combinations of Hewlett-Packard Model 10515A passive doublers and Instruments for Industry wide-band amplifiers. The output of this system is then amplified by a Hewlett-Packard type 230A tuned amplifier capable of 4-W output. The final microwave frequencies are reached by using varactor diodes to multiply the frequency in order to drive an appropriate microwave travelling-wave amplifier. Tuning stubs were inserted in the line wherever necessary to select the proper harmonics. The region 1–3 GHz was scanned with a cavity wavemeter to guarantee that the equipment was tuned to the desired frequency and that spurious harmonics had been suppressed. Thus, the frequency of the signal fed to the hairpin was known to approximately 1 part in 10<sup>8</sup>, and was stable to a few parts in 10<sup>9</sup>. When frequency was swept, the output of the synthesizer was monitored with a Hewlett-Packard Model 524C frequency counter.

The hairpin, a U-shaped copper strap similar to the design illustrated in Fig. 1 of the paper by Woodgate and Hellwarth,<sup>9</sup> can be turned through 90° to excite either  $\pi$  or  $\sigma$  transitions. The same loop was used both for the microwave transitions

and for the low-frequency field-calibrating transitions.

#### IV. EXPERIMENTAL PROCEDURE

In our apparatus there is at least one focusable  $\Delta F=1$ ,  $\Delta M=0$  transition between each of the four zero-field levels of the ground state of bismuth. From the data of Title and Smith, who measured two of these transitions, we estimated the location of the third transition  $\nu_3$ .

The frequencies of all three transitions were re-measured in magnetic fields ranging from 1.3 to 5.1 G. In each case the current through the C magnet was set to some value, and the magnetic field was calibrated by measuring the frequency of the low-frequency resonance in the  $F=5$  state. At low fields the two transitions  $\nu_\beta$  and  $\nu_\sigma$  are unresolved. The field dependence of the observed resonance was set equal to the average value of the two transition frequencies obtained from perturbation theory carried to second order. Title and Smith's value<sup>1</sup> of the electron  $g$  factor ( $g_J = -1.6433$ ) was used in this analysis. A series of measurements was then made sandwiching the high-frequency  $\Delta F=1$  measurements between a pair of field-calibrating low-frequency measurements. The magnetic-field strength was held fixed while the frequency was swept through resonance. In the worst case, field drifts amounted to 20 mG over the entire time of the measurements made at a given field and, typically, were approximately 5 mG.

A total of 33 observations of the three direct transitions at four different magnetic-field strengths was used to determine the zero-field hyperfine intervals. A computer program, adapted from the Berkeley program<sup>10</sup> hyperfine 4-94 for our CDC 6400 computer, was used to provide a best least-squares fit to the data by varying the three hyperfine parameters  $A$ ,  $B$ , and  $C$ . The resonance  $\nu_3$ ,  $(3,0) \rightarrow (4,0)$ , is displayed in Fig. 3 as an example of our data. The average line width was about 40 KHz for the two field-independent transitions  $(3,0) \rightarrow (4,0)$  and  $(4,0) \rightarrow (5,0)$ , which is the width expected from our 1-cm-long rf hairpin. The  $(5,4) \rightarrow (6,4)$  transition ( $\nu_1$ ) is broader, probably due to magnetic-field inhomogeneities. The error in the frequency measurement was chosen as the uncertainty in locating the line center. This uncertainty was caused by irregularities (noise) in the line shape and usually amounted to not more than 3 KHz. Errors in the magnetic-field measurements were arbitrarily assigned between 0.1 and 1% of the field value itself. This variation in field error produced no change in the values of the computed hyperfine-interaction constants to within the errors quoted below. The data were also fit in the least-squares sense to polynomials of first and second degree in  $H$ . Values of the zero-field hyperfine intervals read from these polynomials

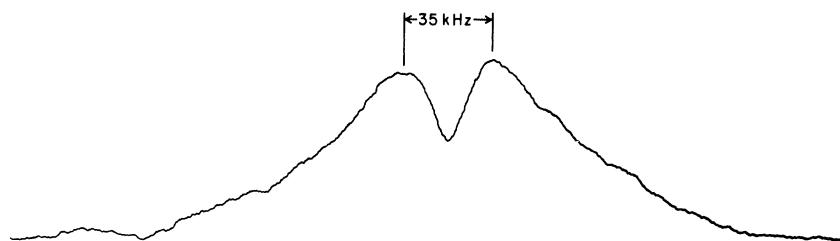


FIG. 3. Resonance corresponding to the  $(4, 0) \rightarrow (5, 0)$  transition ( $\nu_2$ ) observed at a field of a few gauss and a frequency of approximately 2171 MHz. This record was made with a sweep width of about 350 KHz to show the full pattern. The sweep width was reduced to 100 KHz during actual measuring runs to improve accuracy.

agreed with the more elaborate calculations to within a few tenths of a kilohertz.

### V. RESULTS AND DISCUSSION

The zero-field hyperfine intervals in the  $(6p^3)^4S_{3/2}$  state of  $\text{Bi}^{209}$  were obtained from the  $\Delta F=1$ ,  $\Delta M=0$ , observations by computer analysis. The results are (in MHz):

$$\nu_1(F=5 \rightarrow F=6) = 2884.666(2),$$

$$\nu_2(F=4 \rightarrow F=5) = 2171.419(2),$$

$$\nu_3(F=3 \rightarrow F=4) = 1584.502(2).$$

Hyperfine interaction constants deduced from these values are (in MHz):

$$A = -446.942(1), \quad B = -304.654(2), \\ C = 0.0165(1).$$

The computer was programmed to make a simultaneous least-squares fit to the experimentally measured field and frequencies with  $A$ ,  $B$ , and  $C$  treated as free parameters. Electronic and nuclear  $g$  factors were held fixed with  $g_J = -1.6433$  and  $g_I = 4.889 \times 10^{-4}$ , and the value<sup>11</sup> for  $g_I$  is used without diamagnetic correction. Our values for the transition frequencies agree with those measured by Title and Smith.<sup>1</sup> In addition, we have obtained a value for the magnetic octupole-interaction constant.

#### A. Dipole and Quadrupole Interactions

Previous measurements of the dipole- and quadrupole-interaction constants were sufficiently accurate, so that essentially no new information about these interactions is contained in our improved values. Lurio and Landman<sup>2</sup> discuss the results available in 1966 for all states of the  $(6p^3)$  configuration.

#### B. Octupole-Interaction Constant

Second-order terms in the perturbation-theory expansion of the hyperfine energy may be treated

as corrections to the measured zero-field hyperfine-structure intervals. We have evaluated the effects caused by the other states within the  $(6p^3)$  configuration. When the corrections are applied, Eqs. (3) can be solved again for new values of  $A$ ,  $B$ , and  $C$ . Although the second-order corrections require a knowledge of the one-electron hyperfine constants  $a'$ ,  $a''$ ,  $a'''$ , and  $b$ , which in turn are derived from  $A$ ,  $B$ , and  $C$  via Eqs. (6), the effect of the second-order terms is negligible on the dipole and quadrupole constants. Hence, a set of  $a$  and  $b$  values is found with corrections ignored. Then this set is used to calculate the corrections and a new set of  $A$ ,  $B$ , and  $C$  values is found. This last set is called the corrected set in Table II, where the results are listed. We have applied similar corrections to the data of Lurio and Landman<sup>2</sup> for the  $^2P_{3/2}$  state of this configuration and have included both the corrected and uncorrected values in Table II.

We have used for the one-electron interaction constants the values given by Lurio and Landman, who obtained them by treating  $a'$ ,  $a''$ , and  $a'''$  as three independent parameters and fitting them to the five  $A$  values of the five fine-structure states in this configuration. Usually the ratios of these parameters are considered determined by theory, and thus there should be only one free parameter. A value for the quadrupole constant was obtained from data for the entire configuration (only three states should show a quadrupole interaction), and the relativistic correction  $\eta$  was taken to be 1.55.<sup>2</sup> The values of the interaction constants used in evaluating the second-order corrections are (in MHz):  $a' = 363$ ,  $a'' = 11310$ ,  $a''' = -681$ , and  $b = -801$ . The significance of this method of choosing these constants is discussed by Lurio and Landman.

We note that the corrections to  $C$  are approximately 10% of the uncorrected values. These corrections are relatively small in the case of bismuth, owing to the large fine-structure energy differences within the configuration.

#### C. Magnetic Octupole Moment

The magnetic octupole moment  $\Omega$  of the  $\text{Bi}^{209}$  nucleus can be obtained from the following relation-

TABLE II. Uncorrected and corrected values of the observed hyperfine intervals and the interaction constants. All units are MHz. The quoted errors are deduced from the experimental errors in the measurement of the zero-field hyperfine intervals. No estimate of the errors in the theoretical corrections has been made.

	$(6p^3) \ ^4S_{3/2}$		$(6p^3) \ ^2P_{3/2}$	
	Uncorrected	Corrected	Uncorrected <sup>a</sup>	Corrected
$\nu_1$	2884.666(2)	2884.900(2)	3598.647(6)	3598.694(6)
$\nu_2$	2171.419(2)	2171.326(2)	2251.038(19)	2251.057(19)
$\nu_3$	1584.502(2)	1584.188(2)	1311.930(10)	1311.872(10)
$A$	-446.942(1)	-446.937(1)	491.026(2)	491.028(2)
$B$	-304.654(2)	-305.067(2)	978.569(10)	978.638(10)
$C$	0.0165(1)	0.0183(1)	0.0207(10)	0.0186(10)
$c_{3/2}$	0.0200(1)	0.0221(1)	0.0212(10)	0.0191(10)

<sup>a</sup>The values in this column are from Ref. 2.

ship given by Schwartz,<sup>3</sup> with relativistic correction  $T$  added:

$$c_{3/2} = \frac{4}{35} \mu_B \Omega |R(r)/r|_{r=0}^2 T. \quad (7)$$

In this expression,  $R(r)$  is the normalized radial part of the electronic wave function. For the  $6p$  electrons in bismuth, we have used the nonrelativistic hydrogenlike radial wave function given by Pauling and Wilson<sup>12</sup> to obtain

$$|R(r)/r|_{r=0}^2 = \frac{70}{34992} \left(\frac{Z}{a_0}\right)^5,$$

where  $a_0$  is the Bohr radius. Ramsey<sup>13</sup> suggests the use of the full unshielded value for the nuclear charge  $Z$ , because the octupole interaction occurs chiefly when the electron is near the nucleus. Thus, we find that  $\Omega = 0.0086 \mu_N b$ , when  $Z = 83$  and  $T = 1.6765$ . However, the derived value of the octupole moment is very sensitive to the choice of  $Z$ . If  $Z = 77$ , as suggested for Bi by Barnes and Smith<sup>4</sup> from an analysis of quadrupole-interaction data, then  $\Omega$  becomes  $0.0135 \mu_N b$ . Both of these values are smaller than the single-particle model prediction<sup>3</sup> of  $0.127 \mu_N b$  for an  $h_{9/2}$  proton. We have used the electron scattering value<sup>15</sup> for the nuclear mean square radius  $\langle r^2 \rangle = 0.304 \times 10^{-24} \text{ cm}^2$  in the single-particle-model prediction. On a plot of octupole moments versus nuclear spins, similar to the Schmidt plot for magnetic dipole moments, our experimental value of  $\Omega$  lies outside the single-particle-model limits.

*Note added in proof.* We have recalculated the value of  $g(0) \equiv |R(r)/r|_{r=0}^2$  by using the numerical wave function for bismuth as given by Herman and Skillman.<sup>18</sup> From their wave function we obtain  $g(0) = 3.9 \times 10^{46} \text{ cm}^{-5}$  with an uncertainty of  $\pm 10\%$ , which depends on the number of tabulated values used in evaluating  $g(0)$ . The calculated octupole moment is  $\Omega = 0.43 \mu_N b$ , which value lies inside the single-particle model limits and closer to the proper limit.

#### ACKNOWLEDGMENTS

The authors wish to acknowledge the encouragement of Dr. James W. Ford, Jr., of the Applied Physics Department of Cornell Aeronautical Laboratory during this work. Thanks are also due to Robert A. Fluegge and James Huber of CAL for their cooperation. We gratefully acknowledge the assistance of Dr. L. C. Bradley, III, with the second-order corrections; Dr. A. Lurio and Dr. D. Landman for generally useful advice and for checking some of our computations; Dr. D. A. Evans for adapting some of the routines of Hyperfine 4-94 for use on our CDC 6400 computer; and Dr. M. Fuda, Dr. T. Sarachman, Dr. L. Wijnberg, and Dr. M. Rustgi for helpful discussions. The computation for this research was done at the Computing Center at the State University of New York at Buffalo, which is partially supported by the National Science Foundation Grant No. Gp 7318.

#### APPENDIX

In order to obtain the second-order corrections to our measured hyperfine-structure intervals, we use the wave functions and coupling coefficients given by Lurio and Landman.<sup>2</sup> The three  $J = \frac{3}{2}$  wave functions are expressed as

$$\psi_i(J = \frac{3}{2}) = a_{si} \psi(^4S_{3/2}) + a_{pi} \psi(^2P_{3/2}) + a_{di} \psi(^2D_{3/2}),$$

in terms of the pure LS wave functions. The coefficients are obtained by fitting the experimental fine-structure energy separations to theory. The values appearing in Table I were obtained with  $F_2 = 990 \text{ cm}^{-1}$  and  $\zeta = 10100 \text{ cm}^{-1}$ , where the quantities  $F_2$  and  $\zeta$  are the electrostatic and spin-orbit parameters, respectively. The  $jj$  basis wave functions are given by Crawford and Wills<sup>16</sup>:

$$\left(\frac{3}{2}, \frac{3}{2}, \frac{3}{2}\right)_{3/2}^{3/2} = (6)^{-1/2} (p_{3/2}^{3/2} p_{3/2}^{1/2} p_{3/2}^{-1/2}),$$

$$\left(\frac{3}{2}, \frac{3}{2}, \frac{1}{2}\right)_{3/2}^{3/2} = (30)^{-1/2} (p_{3/2}^{3/2} p_{3/2}^{-1/2} p_{1/2}^{1/2}) - 2/(30)^{1/2} (p_{3/2}^{3/2} p_{3/2}^{1/2} p_{1/2}^{-1/2}),$$

$$\left(\frac{3}{2}, \frac{1}{2}, \frac{1}{2}\right)_{3/2}^{3/2} = (6)^{-1/2} (p_{3/2}^{3/2} p_{1/2}^{-1/2} p_{1/2}^{1/2}).$$

The three  $J = \frac{3}{2}$  wave functions in terms of these are

$$\psi_i(J = \frac{3}{2}) = c_{1i} \left(\frac{3}{2}, \frac{3}{2}, \frac{3}{2}\right)_{3/2}^{3/2} + c_{2i} \left(\frac{3}{2}, \frac{3}{2}, \frac{1}{2}\right)_{3/2}^{3/2} + c_{3i} \left(\frac{3}{2}, \frac{1}{2}, \frac{1}{2}\right)_{3/2}^{3/2}.$$

Reduced matrix elements of the dipole and quadrupole tensor operators  $T_e^{(k)}$  ( $k=1, 2$ ) operating in the space of electronic coordinates are given below. The notation is that of Schwartz.<sup>3</sup> The single-electron matrix elements were taken from Lurio, Mandel, and Novick<sup>4</sup>:

$$\langle \psi_i(J = \frac{3}{2}) | T_e^{(1)} | \psi_j(J = \frac{3}{2}) \rangle$$

$$= (15)^{1/2} [(c_{1i} c_{1j} + \frac{6}{5} c_{2i} c_{2j} + c_{3i} c_{3j}) a' - \frac{1}{5} c_{2i} c_{2j} a'' - (c_{1i} c_{2j} + c_{2i} c_{1j} - c_{2i} c_{3j} - c_{3i} c_{2j}) 2(\frac{2}{5})^{1/2} a'''] I / \mu_I;$$

$$\langle \psi_i(J = \frac{3}{2}) | T_e^{(2)} | \psi_j(J = \frac{3}{2}) \rangle$$

$$= [c_{3i} c_{3j} - c_{1i} c_{1j} - (\frac{2}{5})^{1/2} \eta (c_{1i} c_{2j} + c_{2i} c_{1j} + c_{2i} c_{3j} + c_{3i} c_{2j})] (5)^{1/2} b / Q;$$

$$\langle \psi_i(J = \frac{3}{2}) | T_e^{(1)} | \psi(^2D_{5/2}) \rangle$$

$$= [(c_{1i} - c_{3i}) a''' + c_{2i} (a' - a'') (\frac{2}{5})^{1/2}] (6)^{1/2} I / \mu_I;$$

$$\langle \psi_i(J = \frac{3}{2}) | T_e^{(2)} | \psi(^2D_{5/2}) \rangle = -(\frac{21}{2})^{1/2} \eta b (c_{1i} + c_{3i}) / Q;$$

$$\langle \psi_i(J = \frac{3}{2}) | T_e^{(1)} | \psi(^2P_{1/2}) \rangle = - (6)^{1/2} a''' (c_{1i} + c_{3i}) I / \mu_I;$$

$$\langle \psi_i(J = \frac{3}{2}) | T_e^{(2)} | \psi(^2P_{1/2}) \rangle = (10)^{1/2} [\frac{1}{2} (c_{1i} - c_{3i}) \eta + 2c_{2i}] b / Q.$$

The  $a'$ ,  $a''$ , and  $a'''$  are the magnetic dipole-interaction constants defined by Breit and Wills,<sup>17</sup> and  $\eta$  is a relativistic correction.<sup>3</sup>

\* Present address: Massachusetts Institute of Technology Lincoln Laboratory, Lexington, Mass. 02173.

<sup>1</sup>R. S. Title and K. F. Smith, *Phil. Mag.* **5**, 1281 (1960).

<sup>2</sup>A. Lurio and D. A. Landman, *La Structure Hyperfine Magnetique des Atomes et des Molecules* (Editions du Centre National de la Recherche Scientifique, Paris, 1967), p. 211.

<sup>3</sup>C. Schwartz, *Phys. Rev.* **97**, 380 (1955).

<sup>4</sup>A. Lurio, M. Mandel, and R. Novick, *Phys. Rev.* **126**, 1758 (1962).

<sup>5</sup>M. Posner, Princeton University Technical Report No. NYO-2966, 1961 (unpublished).

<sup>6</sup>S. Mrozowski, *Phys. Rev.* **62**, 526 (1942).

<sup>7</sup>G. O. Brink, *Rev. Sci. Instr.* **37**, 857 (1966).

<sup>8</sup>M. P. Klein and G. W. Barton, Jr., *Rev. Sci. Instr.* **34**, 754 (1963).



<sup>9</sup>G. K. Woodgate and R. W. Hellwarth, Proc. Phys. Soc. (London) **A69**, 588 (1956).

<sup>10</sup>We wish to thank Professor Howard A. Shugart for a copy of the program Hyperfine 4-94 and for advice on its use. A description of the computational methods used in this program appears in the paper by V. J. Ehlers, Y. Kabasakal, H. A. Shugart, and O. Tezer [Phys. Rev. **176**, 25 (1968)].

<sup>11</sup>W. G. Proctor and F. C. Yu, Phys. Rev. **78**, 471 (1950).

<sup>12</sup>L. Pauling and E. B. Wilson, Jr., Introduction to Quantum Mechanics (McGraw-Hill Book Co., Inc., New York, 1935), p. 136.

<sup>13</sup>N. F. Ramsey, Molecular Beams (Oxford University Press, London, 1963), p. 279.

<sup>14</sup>R. G. Barnes and W. V. Smith, Phys. Rev. **93**, 95 (1954).

<sup>15</sup>G. J. C. Van Niftrik and R. Engfer, Phys. Letters **22**, 490 (1966).

<sup>16</sup>M. F. Crawford and L. A. Wills, Phys. Rev. **48**, 69 (1935).

<sup>17</sup>G. Breit and L. A. Wills, Phys. Rev. **44**, 470 (1933).

<sup>18</sup>F. Herman and S. Skillman, Atomic Structure Calculations (Prentice-Hall, Englewood Cliffs, N. J., 1963), pp. 6-204.

PHYSICAL REVIEW A

VOLUME 1, NUMBER 3

MARCH 1970

## Stimulated Electric Polarization and Photon Echoes\*

C. V. Heer and R. H. Kohl

*Department of Physics, Ohio State University, Columbus, Ohio 43210*

(Received 20 August 1969)

The change in the wave function of an atom or molecule which interacts with saturating incident radiation is shown to have a time evolution operator  $U(t, 0) = \sum |n\rangle \langle n'| B(n\alpha) B^*(n'\alpha) \times e^{-i[\xi(n\alpha) + E(n)/\hbar]t}$ , where the sum over  $n$  and  $n'$  is over both the  $(2J_a + 1)$  values of  $m_a$  and  $(2J_b + 1)$  values of  $m_b$ , and the sum over  $\alpha$  is over the  $(2J_a + 1) + (2J_b + 1)$  modes indicated by the index  $\alpha$ . The eigenvalues  $\xi(n\alpha)$  and their eigenvectors  $B(n\alpha)$  depend on the intensity and polarization of the incident radiation, produce a modulation term in the electric polarization  $\vec{P}$  of the molecule, and give rise to anomalous polarization in the stimulated radiation. This unitary operator is used to discuss the radiation stimulated by two pulses or photon echoes. Echoes from elliptical pulses are discussed for  $J \leq 2$ , and the linear-linear sequence is compared with the theory of Gordon, Wang, Patel, Slusher, and Tomlinson. Echoes from linear-circular and circular-linear pulse sequences are discussed in detail.

### I. INTRODUCTION

The anomalous response of an atom or molecule to an intense radiation field is of considerable interest for the anomalous polarization which occurs in laser radiation,<sup>1,2</sup> the anomalous polarization which occurs in the cosmic OH emission,<sup>3</sup> and in the polarization phenomena which occurs in photon echoes.<sup>4,5</sup> The earlier calculations<sup>1</sup> for lasers were made using a perturbation approach and lead to the interesting conclusion that a laser operating between a  $J_a = 2 \leftrightarrow J_b = 2$  transition prefers circular polarization, while a  $J_a = 2 \leftrightarrow J_b = 1$  laser prefers linear.<sup>6</sup> Photon echoes occur in the region in which the perturbation approach is no longer appropriate.

This paper uses an approach which permits the discussion of radiation fields which are so strong that a perturbation approach is not appropriate. The interaction of an atom or molecule with a single frequency time-dependent potential  $V(t)$  for a finite time interval is considered. If this interaction is between energy levels with degeneracies

of  $(2J_a + 1)$  and  $(2J_b + 1)$ , the problem can be discussed in terms of  $(2J_a + 1) + (2J_b + 1)$  modes. These modes have eigenvalues which depend on the nature and strength of the interaction. A time evolution operator is developed and tables of coefficients are given for all electric and magnetic dipole transitions for  $J \leq 2$ . The electric polarization of the atom or molecule, which is stimulated by the radiation field, is given in terms of the time evolution operator. This development permits the discussion of the intensity and elliptical polarization of photon echoes with arbitrary polarization for the first and second pulses. A detailed discussion is given for linear-linear, linear-circular, and circular-linear sequence of pulses for  $J \leq 2$ . The linear-linear effects are in agreement with the very elegant operator development of Gordon *et al.*<sup>4</sup> Linear-circular or circular-linear have distinctive features in the echo intensities and should yield an assignment of the  $J$  values of the transitions.

Since the development in this paper treats the interaction as the addition of a time-dependent